Electronic Supplementary Material (ESI) for Chemical Communications

2D and 3D Photoreactive Lanthanide MOFs of trans,trans-muconic acid

Adonis Michaelides*, Stavroula Skoulika and Michael G. Siskos

Department of Chemistry, University of Ioannina, 45110 Ioannina, Greece

Supporting Information

Experimental

Syntheses

(a) Gel synthesis: An aqueous suspension of H_2Hex (0.710 g in 60 ml of water) was brought to pH 5.8 by means of a sodium silicate solution (d=1.06). The resulting gelling solution was distributed in six test tubes and was allowed to stand for about three days. Then, an aqueous solution of $ErCl_3$ (or YCl_3) 0.07 M was carefully poured at the top of each silica gel column. The volume of the aqueous metal solution was equal to the volume of the gel column. Under these conditions, aggregated crystals of compound **3 (**or **4** if Y^{3+} is used) are formed within 2-3 days. By repeting this experiment many times (some hundreds of tubes) we observed that, in some cases, a few well-shaped crystals of **1**[1] or **3** or **5** (**2** or **4** or **6** when Y^{3+} is used), appear at the gel-solution interface after about 10 days. Upon prolonged growth time (more than four weeks) the aggregated crystals of 3 (or 4), formed initially in the gel column transform into phase **7** (or **8** if Y^{3+} is used) which appears as aggregated microcrystals.

(b) Precipitation reaction: This technique was used to prepare powdered phases **5** and **6** in large quantities. An aqueous suspension of H_2Hex (0.710 g in 60 ml of water) was brought to pH 5.8 by means of NaOH pellets and then was mixed with an equal volume of an aqueous solution of $ErCl_3$ (or YCl_3) 0.07 M. The resulting precipitate was **immediately** recovered by filtration.

(c) Hydrothermal reaction: This technique was used to prepare single crystals of **7**. An aqueous suspension of H_2Hex (0.710 g in 60 ml of water) was brought to pH 5.8 by means of NaOH pellets. 5 ml of the resulting solution was transferred in a teflon tube and then was mixed with 5 ml of $ErCl_3$ 0.07 M. The mixture was heated at 90°C for 3 days. Single crystals of **7** in the form of quasi cubic morphology were formed, along with elongated prismatic crystals of another phase photochemically inactive. The analogous reaction with Y^{3+} leads to a new, photochemically active, phase.

Crystal structure determination: The X-ray diffraction data for compounds **3-6** were collected at room temperature, on a Bruker P4 diffractometer, using graphite monochromated MoKα radiation (λ=0.71073 Å). For compound **7** diffraction data

were collected at 100K on a Bruker APEX 2 diffractometer using MoKα radiation (data collection carried out at Bruker lab., Carlsrue, Germany). All data were corrected for Lorentz and polarization effects. The structures were solved by direct methods and refined by full-matrix least-squares techniques using the SHELXL-97 package (Sheldrick, 1997). All heavy atoms have been determined by difference Fourier maps and refined anisotropically. Hydrogen atoms of the ligands have been placed on calculated positions and refined using the riding model. The water hydrogen atoms have been located by difference Fourier maps and refined isotropically with fixed thermal parameter. Refinement of the proton positional parameters in case of compound 3, did not lead to reliable positions for the protons bonded to O1W and consequently these parameters have been kept fixed during refinement. Due to the presence of pairs of cations (high electron density) near the water molecules, refinement of these protons resulted to deformation of the water geometry. For this reason, we restrained the water geometry near theoretical values by using DFIX and DANG.

^{1}H-NMR analysis: NMR spectra were recorded on a Bruker AC-250 spectrometer at 250MHz. The samples used for NMR analysis were treated as follows: a) acidification of a D2O solution of the irradiated solid in order to dissociate the metal-carboxylate bonds. b) Addition of a proper amount of NaOH in order to solubilise the organic acids. c) Elimination of yttrium oxide by filtration. In this step, some amount of the organic acids is probably lost as insoluble yttrium coordination polymers. In the spectra, of irradiated phases **6** and **8**, the protons of the muconate dianion appear at 7.04 and 6.20 ppm, the [2+2] photodimer (**rctt** topology) shows a doublet-doublet band at 6.64 ppm, a doublet at 5.84 ppm, a multiplet at 3.49 ppm and a doublet at 3.20 ppm. The cyclooctadiene dimer (Cope photoproduct) presents two singlets at 5.82 and 3.86 ppm. Finally, two singlets at 2.41 and 2.87 ppm are attributed to the ladderane.
The detailed assignement of chemical shifts of compound **4** (A and B isomers with **rtct** topology) was supported by some preliminary DFT/B3LYP/6-31G(d) calculations, followed by GIAO (gauge-invariant atomic orbital) approach to calculate the magnetic shielding tensors. The B3LYP/6-31G+(d,p) basis was used for these calculations. We found that, while the vinyl protons show almost identical chemical shifts in all [2+2] stereoisomers, the cyclobutane protons chemical shifts, for the A and B isomers, move to lower values in comparison with those of the rctt

stereoisomer. If we consider the pedal motion as the mechanism of favourable orientation of double bonds then we would obtain by topochemical reaction the rttc topology. Ab initio calculations show that, in this case, the proton chemical shifts would be expected to appear at higher values, between 3 and 4 ppm, close to those obtained for the rttc isomer obtained in case of compounds **5** and **6**. The presence of two very weak peaks in this region indicates probably the presence of a very small amount of this compound. We had observed during examination of the crystal structure of compounds **3** and **4** that all short olefin contacts are distributed symmetrically at both sides of each ligand (Fig. S1). But, one can observe that if one pair comes into reactive position the other will move far apart and this might explain why a stepped polymer is not formed. For the same reason we exclude formation of a trimer. Moreover, inspection of the NMR spectrum shows that the ratio of integrated areas of the vinylic protons (e,f) to the methine protons, in the region 2-3.5 ppm, is approximately equal to 1. This value is compatible to dimer formation. In case of trimer formation this value should be 0.5. However, the existence of some very weak peaks in the low ppm region does not exclude formation of traces of the trimer.

Irradiation experiments: Photodimerization reactions were carried out using a high pressure 400W mercury light source. An amount of about 30 mg of the compound was placed between two quartz glass slides and was irradiated with UV-irradiation at both sides of the glass slide for various time intervals. The light of the lamp was focused on the sample through a quartz lens (f =10 cm).

Degree of conversion: a) For compound **4** the degree of conversion according to the NMR experiments is about 20%, obtained after about 1h of irradiation. b) For compound **6** the degree of conversion is about 90% according to the NMR spectroscopy, obtained after about 3h of irradiation. c) For compound **8 t**he degree of conversion is about 80% according to Raman spectroscopy. This is in apparent contradiction with the NMR results which show only 20% of conversion. However, solid state Raman spectra of the same sample, irradiated for 2h, obtained after 2,7 and 10 days after irradiation showed a slow progressive increase of the diagnostic peak at 1640 cm^{-1}. From this result it is clear that a back reaction takes place . This back reaction should take place in a much greater extent in the aqueous phase during dissolution of the sample for NMR spectroscopy. This back reaction does not take

place, at least at the time scale of some days, in case of compound 6. In our opinion, this may be due to the fact that in the latter case the photochemical reaction takes place within a macrocycle in which all atomic movements may take place in a more concerted way, leading to a less strained ladderane than in case of compound 8. For this reason, compound 6, during dissolution, transforms mainly into the photoreaction products while compound 8 transforms mainly into the reactants.

IR spectroscopy-Kinetic experiments: The IR spectra were recorded from KBr pellets (Perkin–Elmer FT-IR Spectrum GX). For the kinetic experiments each pellet contains 2mg of sample and 100 mg of KBr. The pellets are irradiated as a function of time at room temperature (22°C). The irradiation time is too short to modify the temperature of the sample which is also protected by the quartz slice and the focusing lens. In all cases we integrated peaks between two isosbestic points. For each isomorphous pair we integrate the same absorption peak and the rate constants thus obtained can be compared between them with confidence. The estimated error is less than 15% as was obtained by determination of k at three experiments taking place at the same conditions, in case of compounds 7 and 8. We chose this pair of isomorphous compounds in order to ensure that the difference between their rate constants, which is relatively small, is significant. We do observe that the error is much less than the difference between kinetic constants in all pairs of isomorphous compounds studied here. Actually, we try to reduce the estimated error of 15% by better control of experimental parameters (granulometry of the sample, intensity of the lamp, concentration and uniformity of the KBr pellet, choice of spectral region etc).

Theoretical calculations: All DFT calculations were performed using the *Gaussian 03* suite of programs[2]. All possible conformations were optimized at the B3LYP/6-31G (d) level of theory and were confirmed to be energy-minimum structures by frequency calculations. NMR calculations were performed using the GIAO[3-7] (gauge-invariant atomic orbital) method as incorporated in the *Gaussian03* software package. NMR shifts were computed at the B3LYP/6-31+G (d,p) level of theory, on the B3LYP/6-31G(d) optimized structures. Values for the ^{1}H isotropic chemical shifts were referenced to the corresponding values for TMS, calculated at the same level of theory. In order to include the effect of water solvation in the

calculations of chemical shifts, the CCPM (conductant polarized continuum mode model) was used.

References

1. A. Michaelides, S. Skoulika and M. G. Siskos, *Chem. Commun*., **2011**, *47*, 7140.
2. M.J. Frisch, G.W. Trucks, H.B. Schlegel, G.E. Scuseria, M.A. Robb, J.R. Cheeseman, J.A. Montgomery Jr., T. Vreven, K.N. Kudin, J.C. Burant, J.M. Millam, S.S. Iyengar, J. Tomasi, V. Barone, B. Mennucci, M. Cossi, G. Scalmani, N. Rega, G.A. Petersson, H. Nakatsuji, M. Hada, M. Ehara, K. Toyota, R. Fukuda, J. Hasegawa, M. Ishida, T. Nakajima, Y. Honda, O. Kitao, H. Nakai, M. Klene, X. Li, J.E. Knox, H.P. Hratchian, J.B. Cross, V. Bakken, C. Adamo, J. Jaramillo, R. Gomperts, R.E. Stratmann, O. Yazyev, A.J. Austin, R. Cammi, C. Pomelli, J.W. Ochterski, P.Y. Ayala, K. Morokuma, G.A. Voth, P. Salvador, J.J. Dannenberg, V.G. Zakrzewski, S. Dapprich, A.D. Daniels, M.C. Strain, O. Farkas, D.K. Malick, A.D. Rabuck, K. Raghavachari, J.B. Foresman, J.V. Ortiz, Q. Cui, A.G. Baboul, S. Clifford, J. Cioslowski, B.B. Stefanov, G. Liu, A. Liashenko, P. Piskorz, I. Komaromi, R.L. Martin, D.J. Fox, T. Keith, M.A. Al-Laham, C.Y. Peng, A. Nanayakkara, M. Challacombe, P.M.W. Gill, B. Johnson, W. Chen, M.W. Wong, C. Gonzalez, J.A. Pople, gaussian 03, Revision D.01, gaussian, Inc., Wallingford CT, 2004..
3. R. McWeeny, Phys. Rev. 126 (1962) 1028–1034.
4. R. Ditchfield, *Mol. Phys.* 27 (1974) 789–807.
5. K. Wolinski, A.J. Sadlej, *Mol. Phys.* 41 (1980) 1419–1430.
6. K. Wolinski, J.F. Hinton, P. Pulay, *J. Am. Chem. Soc*. 112 (1990) 8251–8260.
7. S. K. Wolff, T. Ziegler, *J Chem. Phys.* 109,(1998) 895.

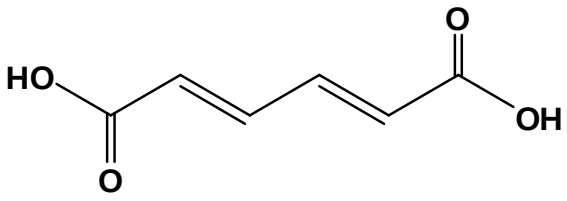

Scheme S1. Trans, trans - muconic acid

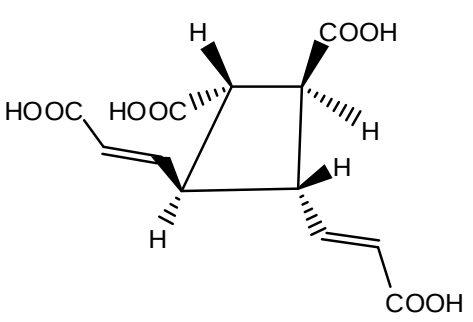

cyclobutane A **(rtct)**

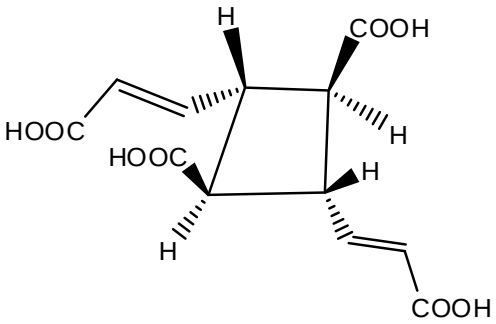

cyclobutane B **(rtct)**

Scheme S2. Conformations of the two possible isomers A and B, obtained by the [2+2] cycloaddition reaction of compound **4**.

Table S1. Crystal and structure refinement data of compounds **3-7**

Compound	**3**	**4**	**5**	**6**	**7**
Empirical formula	$ErC_9H_{16}O_{11}$	$YC_9H_{16}O_{11}$	$Er_2C_{18}H_{28}O_{20}$	$Y_2C_{18}H_{28}O_{20}$	$Er_2C_{18}H_{20}O_{16}$
Formula weight	467.48	389.13	898.92	742.22	826.86
Crystal system	Triclinic	Triclinic	Triclinic	Triclinic	Monoclinic
Wavelemgth (Å)	0.71073	0.71073	0.71073	0.71073	0.71073
Temperature (K)	293(2)	293(2)	293(2)	293(2)	100(2)
Space group	P-1	P-1	P-1	P-1	C2/c
Unit cell dimension (Å) (deg)	*a*= 9.247(2) *b*= 9.437(2) *c*= 9.862(3) α=74.36(2) β= 63.38(2) γ=87.67(2)	*a*= 9.285(1) *b*= 9.468(1) *c*= 9.886(1) α=74.44(1) β= 63.35(1) γ=87.80(1)	*a*= 7.677(1) *b*= 8.018(1) *c*= 22.389(2) α=94.55(1) β= 93.33(1) γ=101.86(1)	*a*= 7.694(1) *b*= 8.033(1) *c*= 22.392(3) α=94.75(1) β= 93.00(1) γ=101.84(1)	*a*= 15.2522(9) *b*= 7.7825(5) *c*= 20.217(2) β= 110.634 (2)
Volume ($Å^3$)	737.7(3)	744.9(1)	1340.6(3)	1346.4(3)	2245.8(3)
Z	2	2	2	2	4
Calculated density (g/cm^{-3})	2.105	1.735	2.227	1.831	2.446
F(000)	452	394	864	748	1568
Reflections collected / unique	3062/2557 [*R*(int) =0.0525]	3076/ 2566 [*R*(int) =0.0251]	5883/ 4730 [R(int) = 0.0221]	5832/ 4705 [R(int) = 0.0444]	9139/ 1980 [R(int) = 0.0264]
Completeness to 2θ	98.8%	98.2%	99.9%	99.0%	99.5%
Goodness-of-fit	1.150	1.030	1.110	0.995	1.240
Final R indices [I>2σ(I)]	R_1 = 0.0380 wR_2 = 0.1207	R_1 = 0.0460 wR_2 = 0.1150	R_1 = 0.0360 wR2 = 0.1000	R_1 = 0.0411 wR2 = 0.0862	R_1 = 0.0152 wR2 = 0.0356

Table S2. Geometric characteristics of the photochemically reactive double bonds

compound	**center-to-center distance (Å)**	**rotation angle* (°)**	**interplanar** angle (°)**
3	3.93	92	53
4	3.94	91	51
5	3.76 3.79	27. 36	70 77
6	3.73 3.78	28 35	72 77
7	3.76 4.04	35 34	60 58

* and **correspond to angles θ1 and θ3 as defined in ref.: V. Ramamurthy and V. Venkatesan, *Chem. Rev.*, **1987**, *87*, 433;

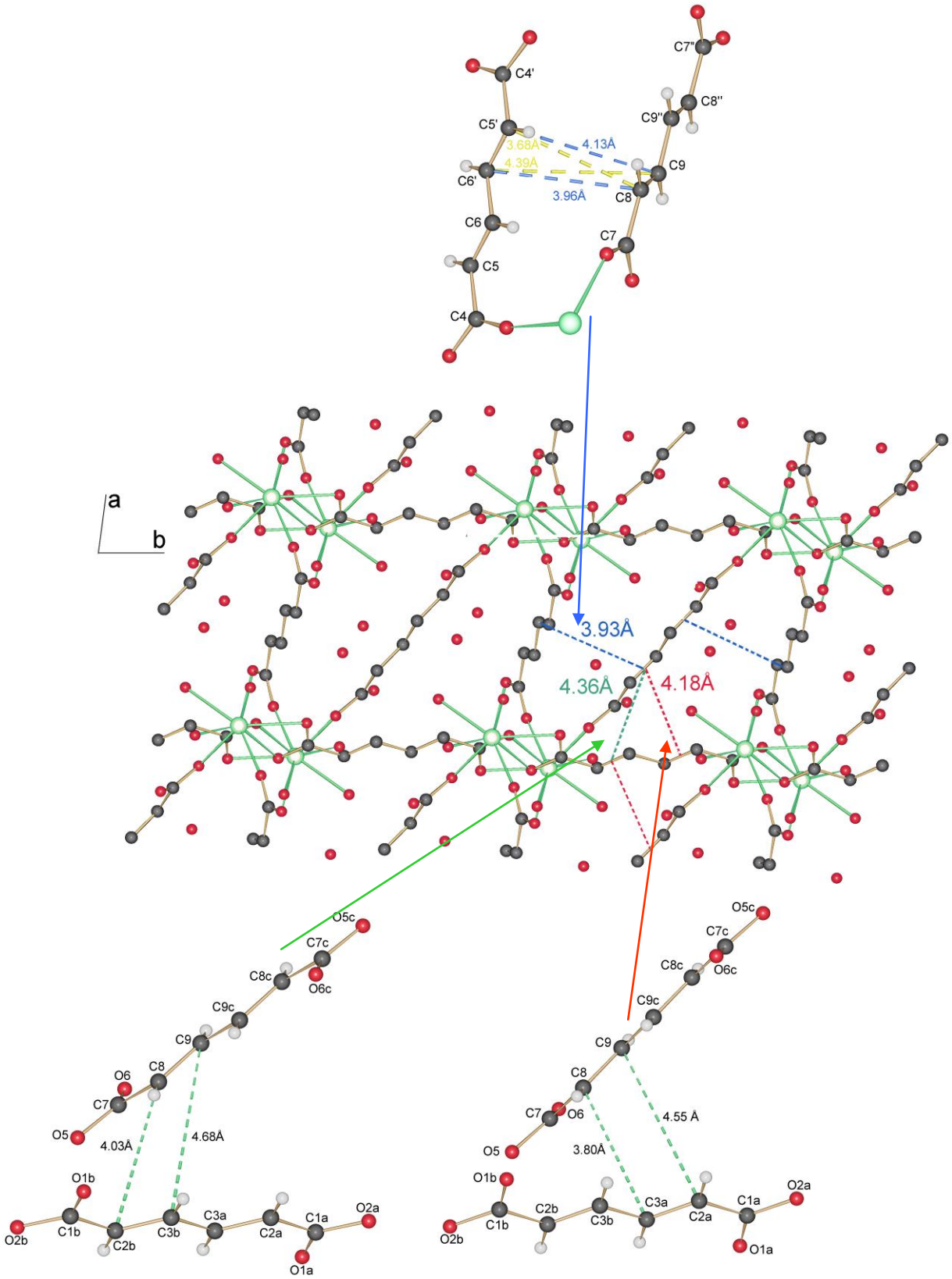

Figure S1. Middle: Projection of the structure of compound **4** along *c*. The blue, red and green dashed lines connect the centers of the double bonds with distances 3.93, 4.18 and 4.36 Å respectively. The atom connectivity leading probably to cyclobutane formation in each case, is shown. All isomers are of the rtct topology . Symmetry codes: (') -x,1-y,1-z; (") -x,2-y,1-z; (a) x,1+y,z; (b) 1-x,1-y,1-z; (c) –x,2-y,1-z

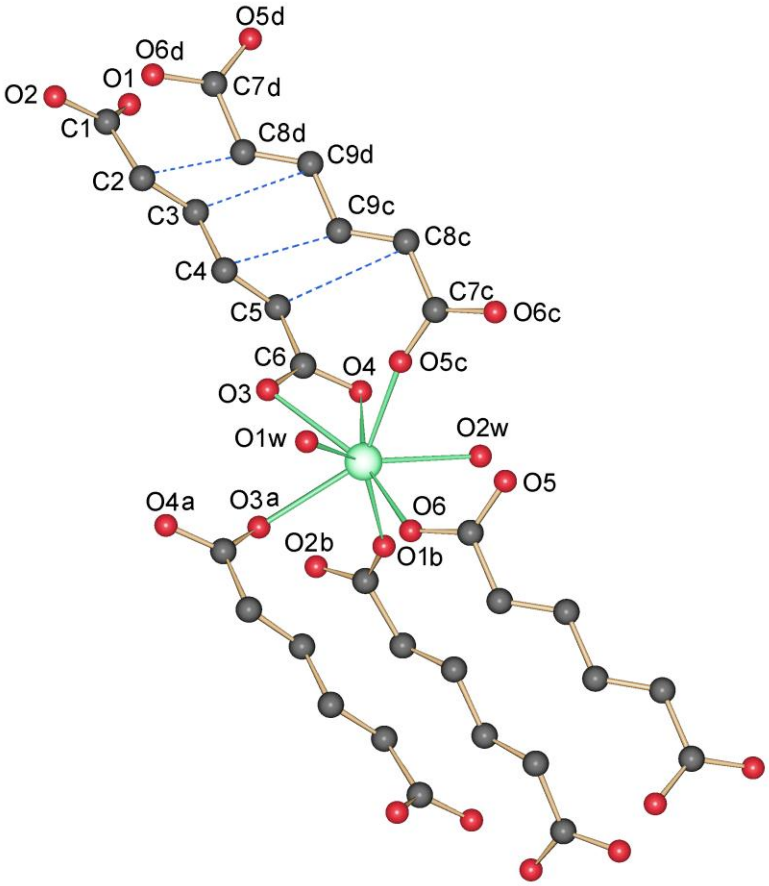

Figure S2. Full coordination geometry of compound 7. The asymmetric unit contains one Er cation, two water molecules, one muconate ligand in general position and half of a second muconate ligand lying about a twofold axis at the center of the C9-C9' bond (C9' generated by the [2-x,y,3/2-z] operation). Symmetry codes: (a) 1-x,1-y,1-z; (b) 0.5+x,0.5-y,0.5+z; (c) 1.5-x,1.5-y,1-z; (d) -0.5+x,1.5-y,-0.5+z.

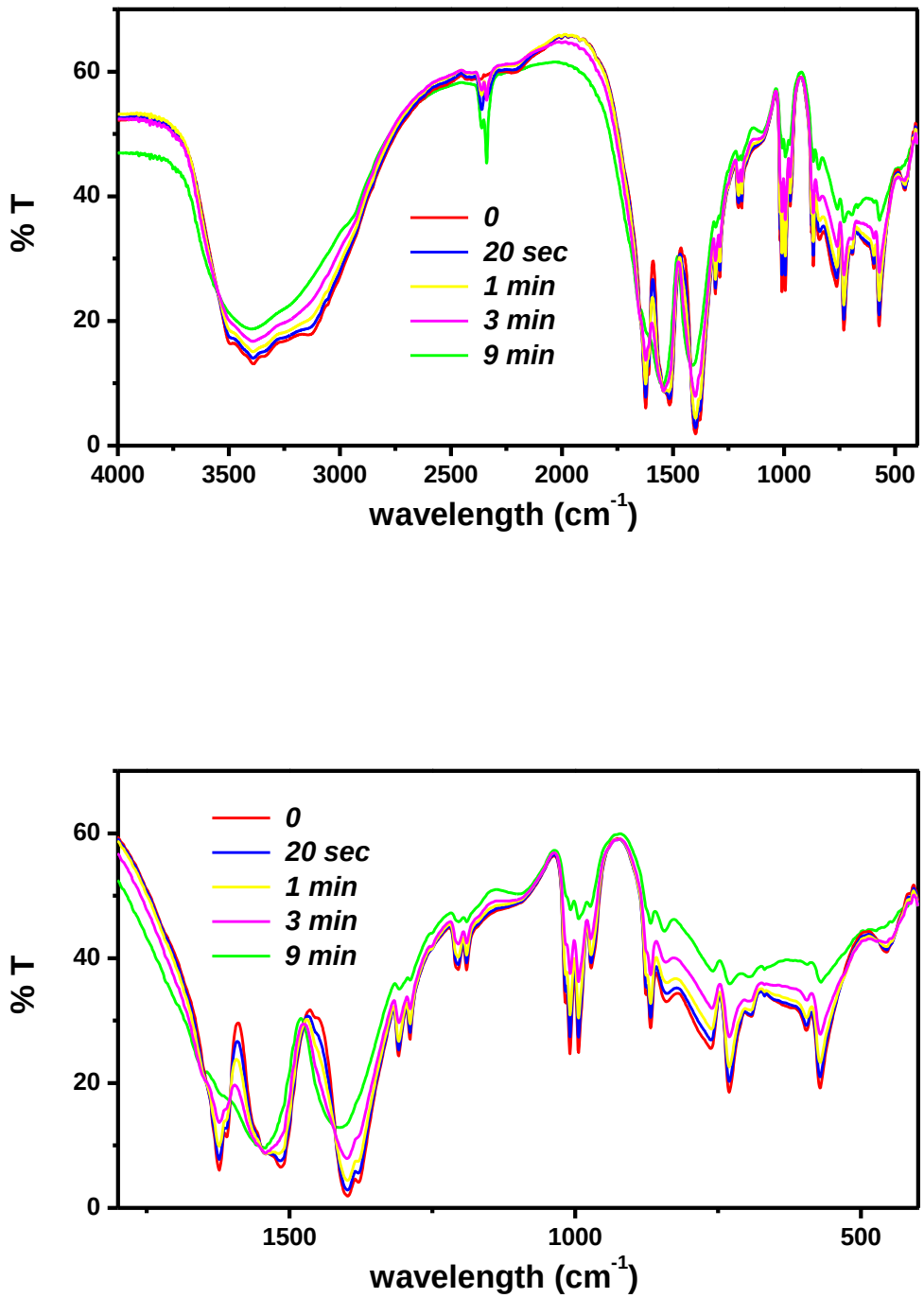

Fig.S3: FT-IR spectrum of compound **3**(KBr pellet) after irradiation with high-pressure 400 W mercury lamp at various time intervals. Full spectrum (*upper figure*) and 1800-400 cm^{-1} wavelength range (*down figure*)

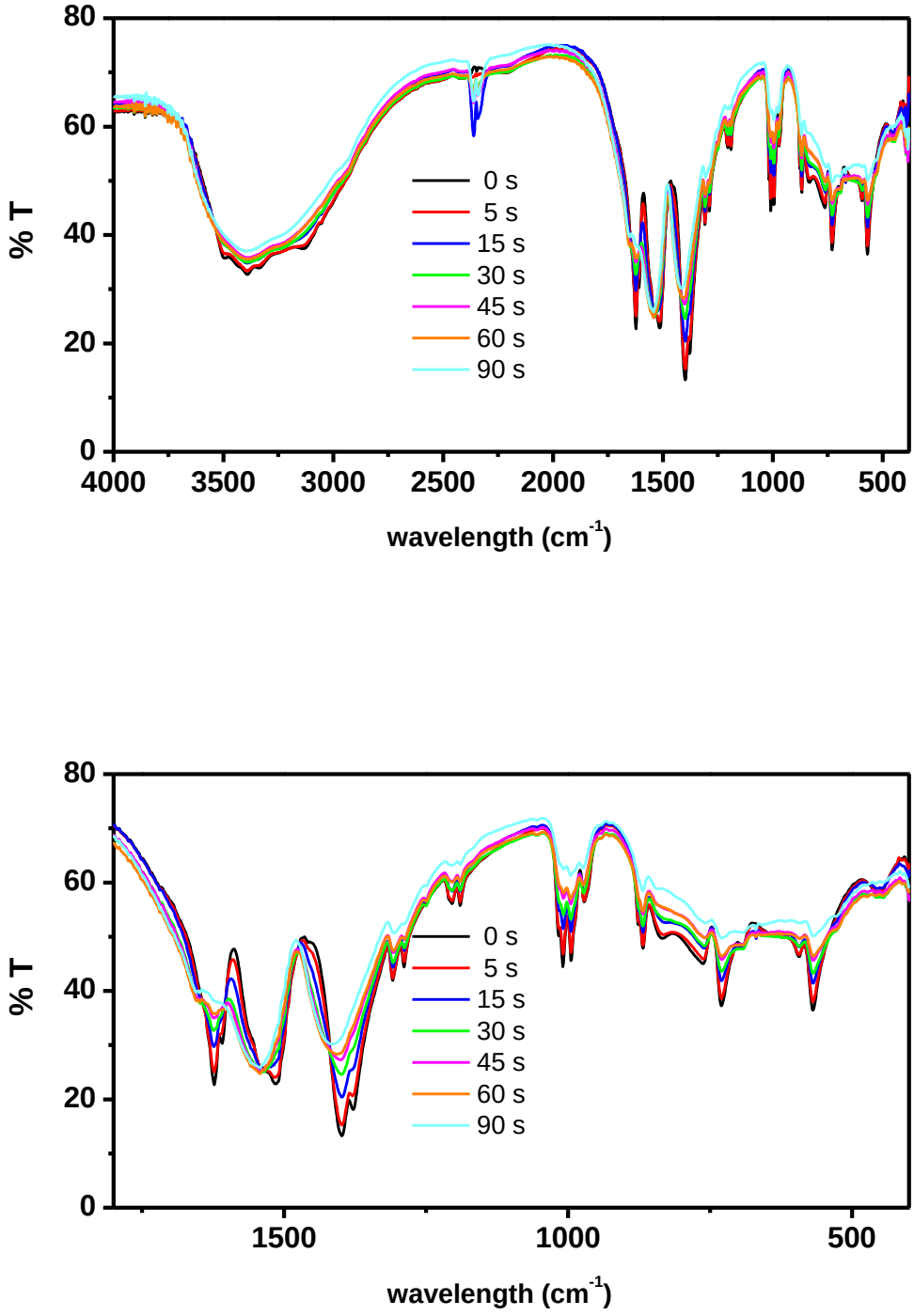

Fig.S4: FT-IR spectrum of compound **4**(KBr pellet) after irradiation with high-pressure 400 W mercury lamp at various time intervals. Full spectrum (*upper figure*) and 1800-400 cm^{-1} wavelength range (*down figure*)

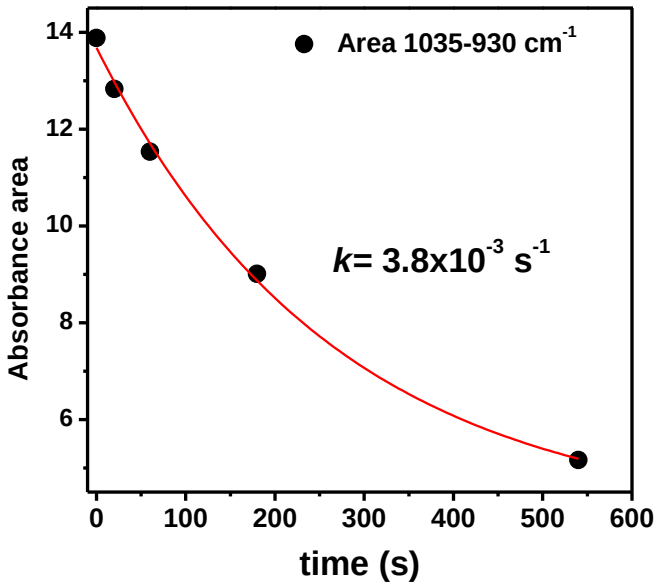

Fig.S5: Irradiation time dependence of the absorbance of a selected band in the FT-IR spectrum, monitored during the photochemically induced dimerization of compound **3**. The rate constant k determined from the decay curve is given.

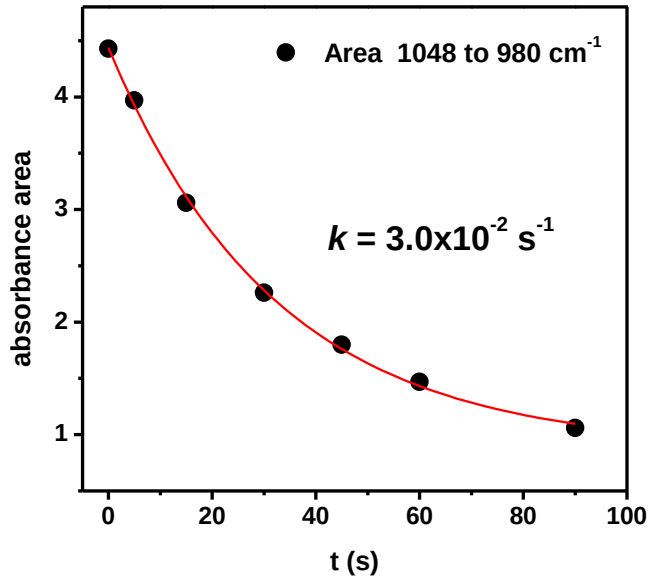

Fig.S6: Irradiation time dependence of the absorbance of a selected band in the FT-IR spectrum, monitored during the photochemically induced dimerization of compound **4**. The rate constant k determined from the decay curve is given.

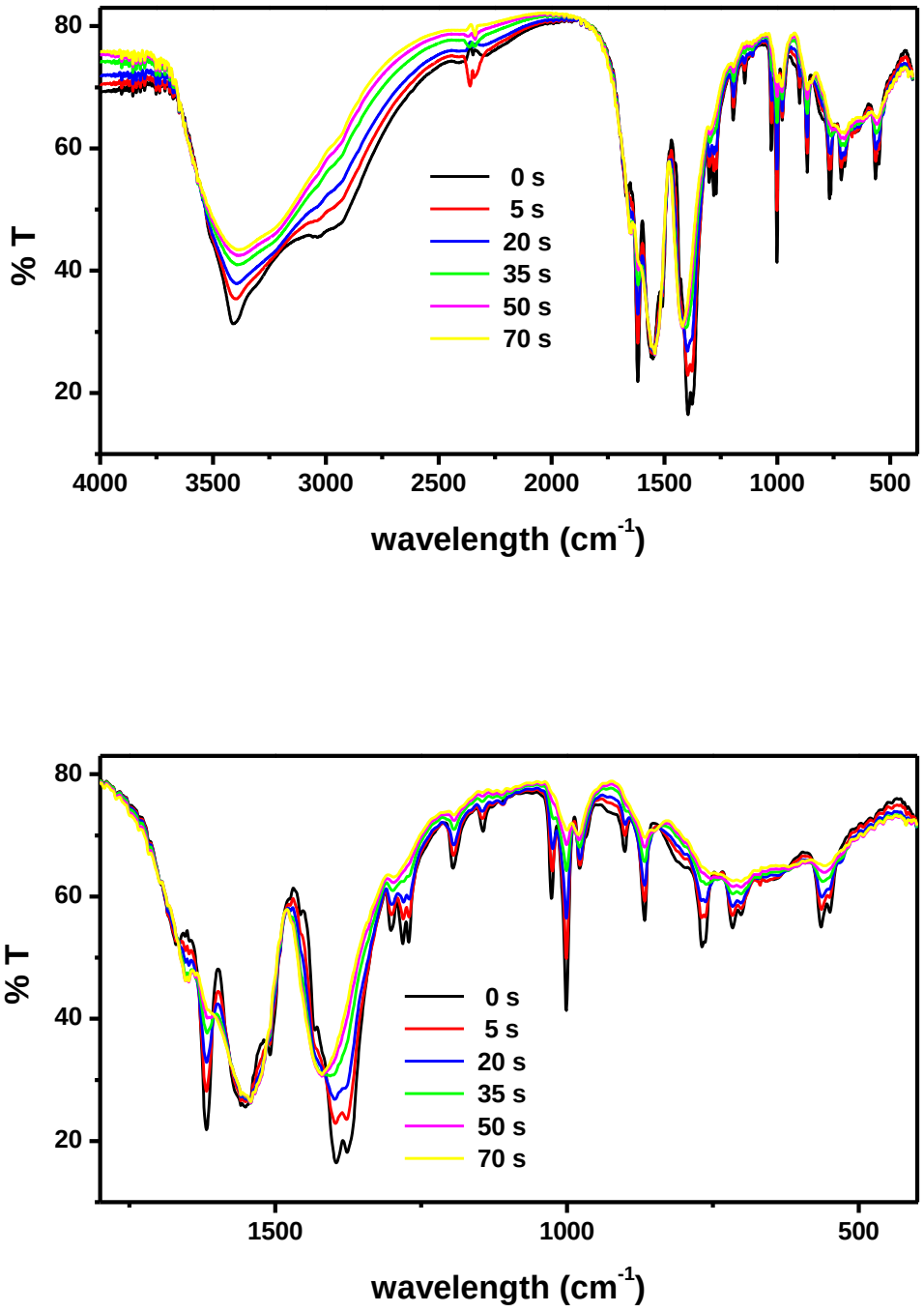

Fig.S7: FT-IR spectrum of compound **5**(KBr pellet) after irradiation with high-pressure 400 W mercury lamp at various time intervals. Full spectrum (*upper figure*) and 1800-400 cm^{-1} wavelength range (*down figure*)

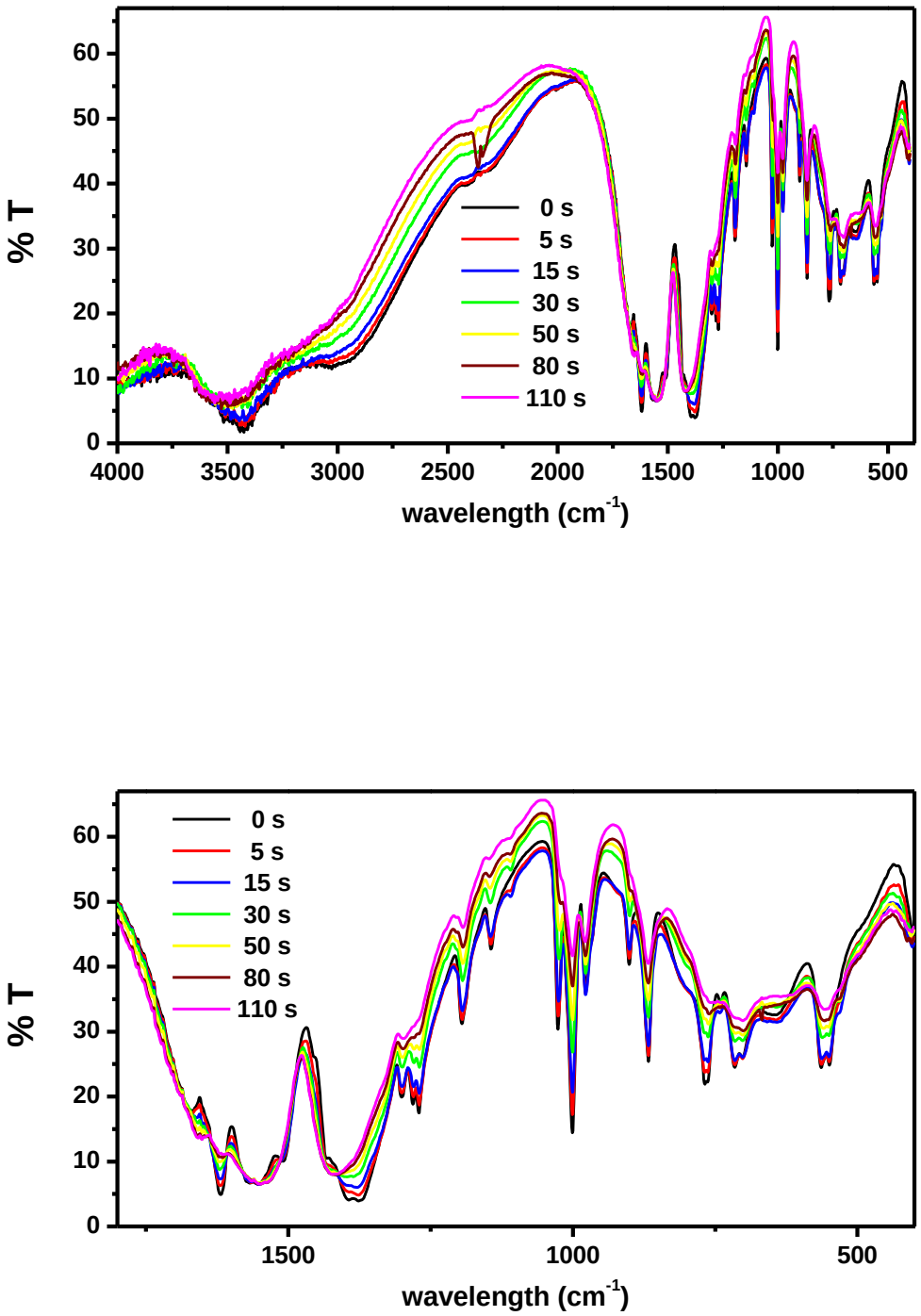

Fig.S8: FT-IR spectrum of compound **6**(KBr pellet) after irradiation with high-pressure 400 W mercury lamp at various time intervals (*using 32.5 % neutral filter*). Full spectrum (*upper figure*) and 1800-400 cm^{-1} wavelength range (*down figure*)

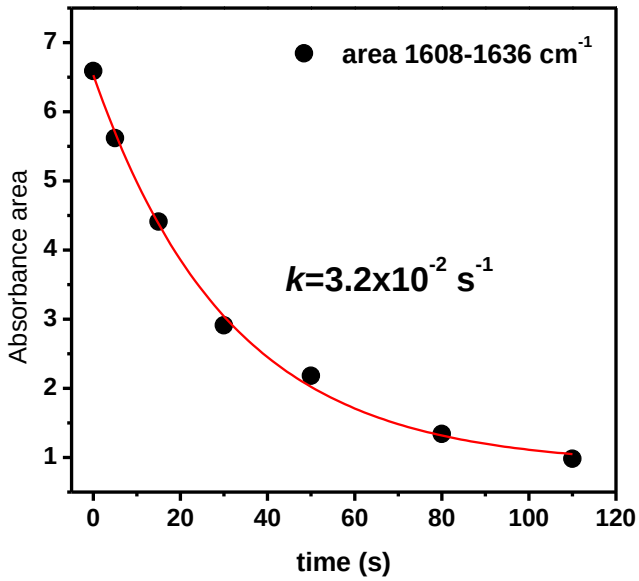

Fig.S9: Irradiation time dependence of the absorbance of a selected band in the FT-IR spectrum, monitored during the photochemically induced dimerization of compound **5**. The rate constant k determined from the decay curve is given.

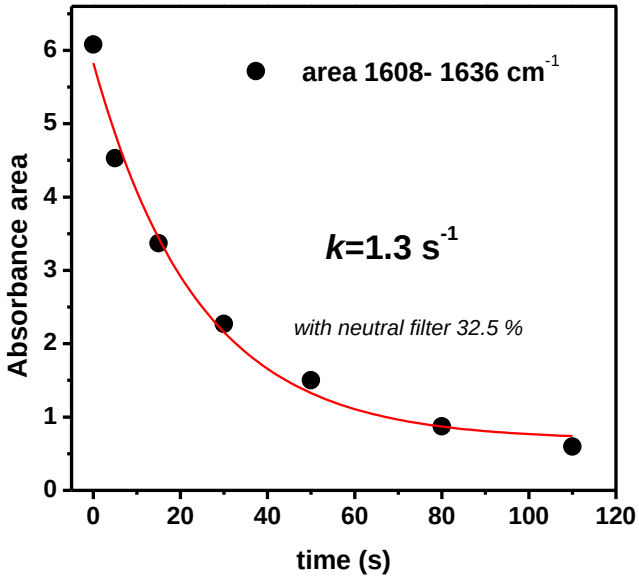

Fig.S10: Irradiation time dependence of the absorbance of a selected band in the FT-IR spectrum, monitored during the photochemically induced dimerization of compound **6**. The rate constant k determined from the decay curve is given.

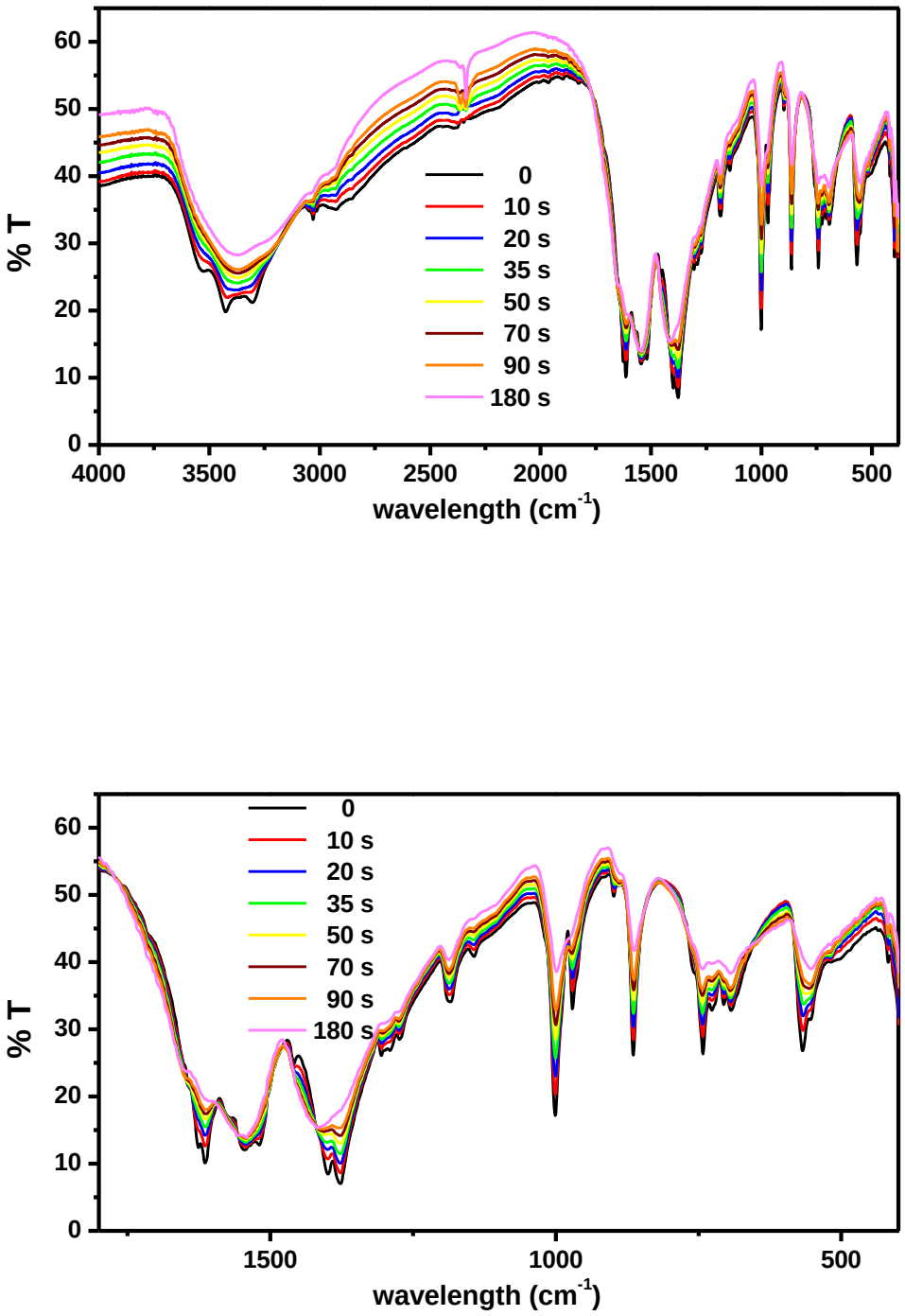

Fig.S11: FT-IR spectrum of compound **7**(KBr pellet) after irradiation with high-pressure 400 W mercury lamp at various time intervals. Full spectrum (*upper figure*) and 1800-400 cm^{-1} wavelength range (*down figure*)

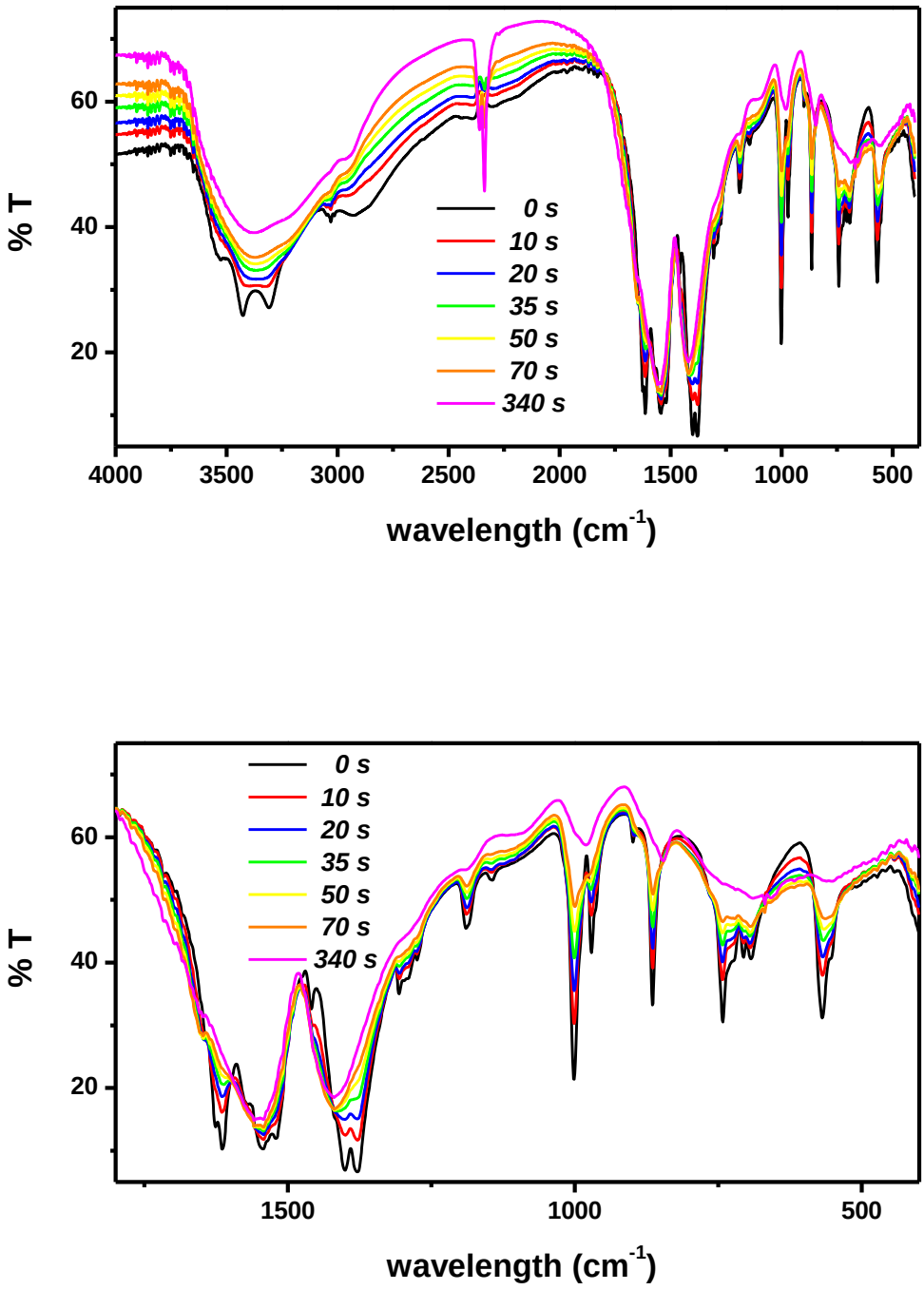

Fig.S12: FT-IR spectrum of compound **8** (KBr pellet) after irradiation with high-pressure 400 W mercury lamp at various time intervals. Full spectrum (*upper figure*) and 1800-400 cm^{-1} wavelength range (*down figure*)

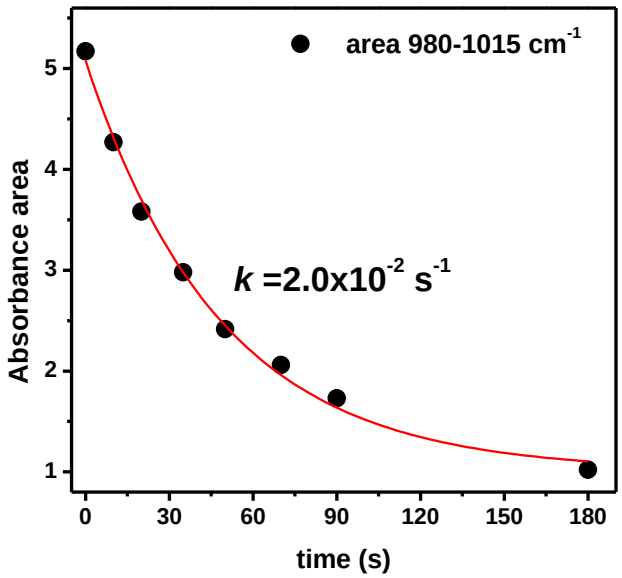

Fig.S13: Irradiation time dependence of the absorbance of a selected band in the FT-IR spectrum, monitored during the photochemically induced dimerization of compound **7**. The rate constant k determined from the decay curve is given.

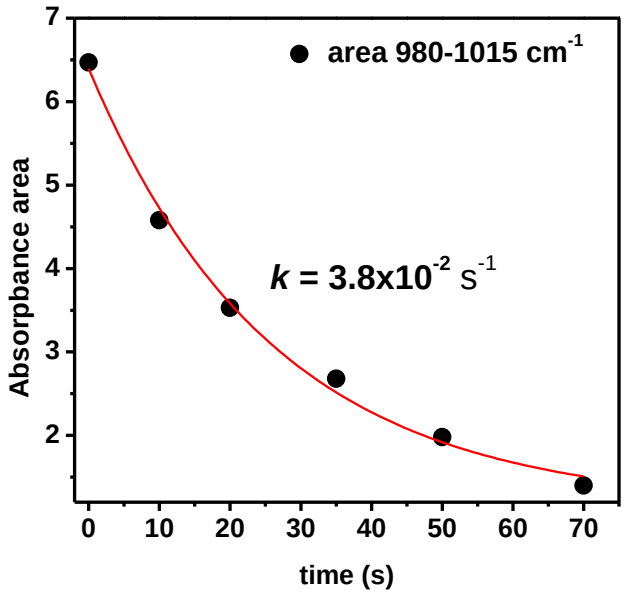

Fig.S14 Irradiation time dependence of the absorbance of a selected band in the FT-IR spectrum, monitored during the photochemically induced dimerization of compound **8**. The rate constant k determined from the decay curve is given.

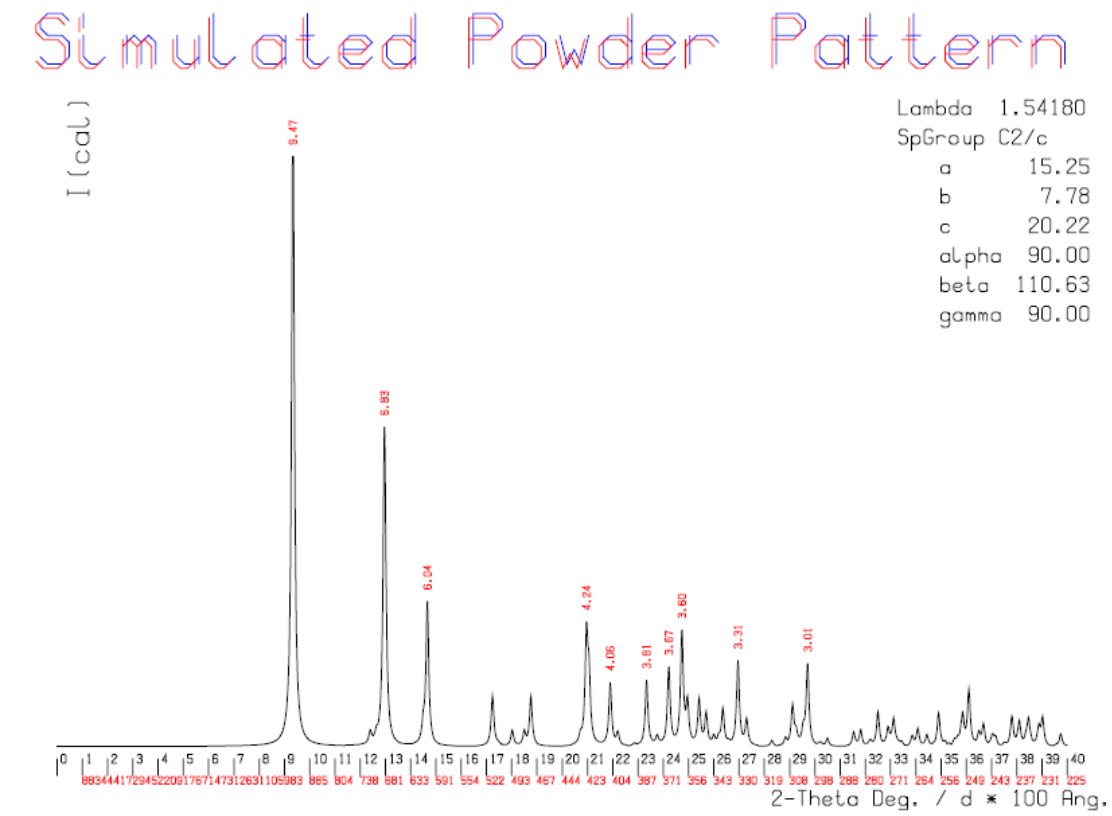

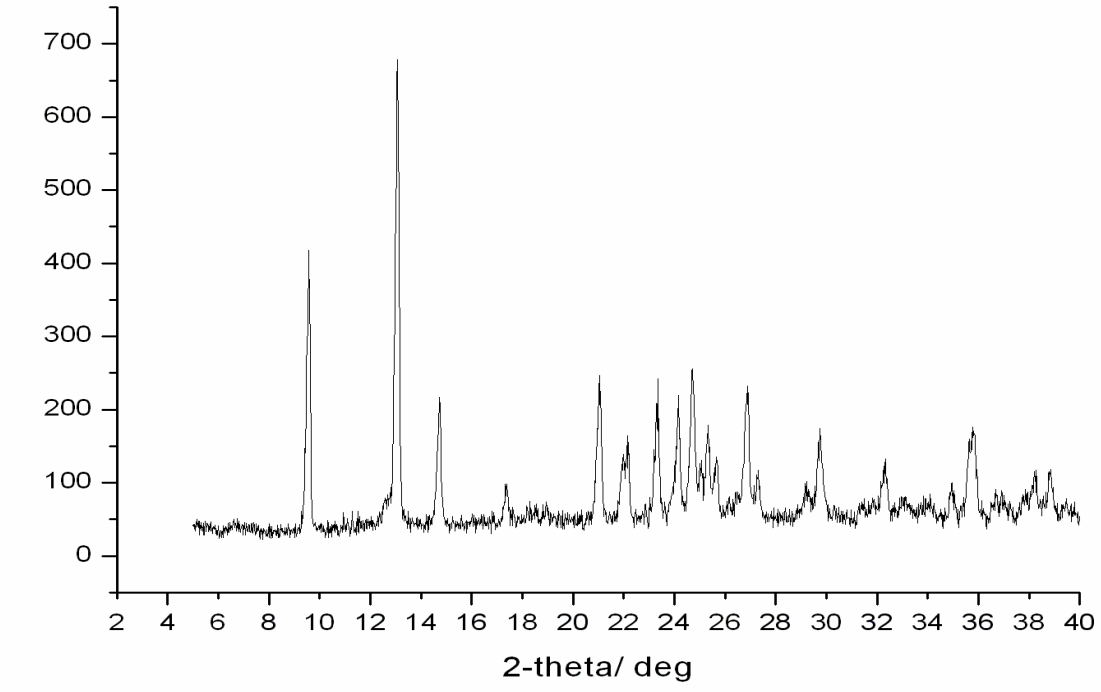

Figure S15. Simulated XRPD pattern of compound **7** (up). Experimental XRPD pattern of compound **8** (down).

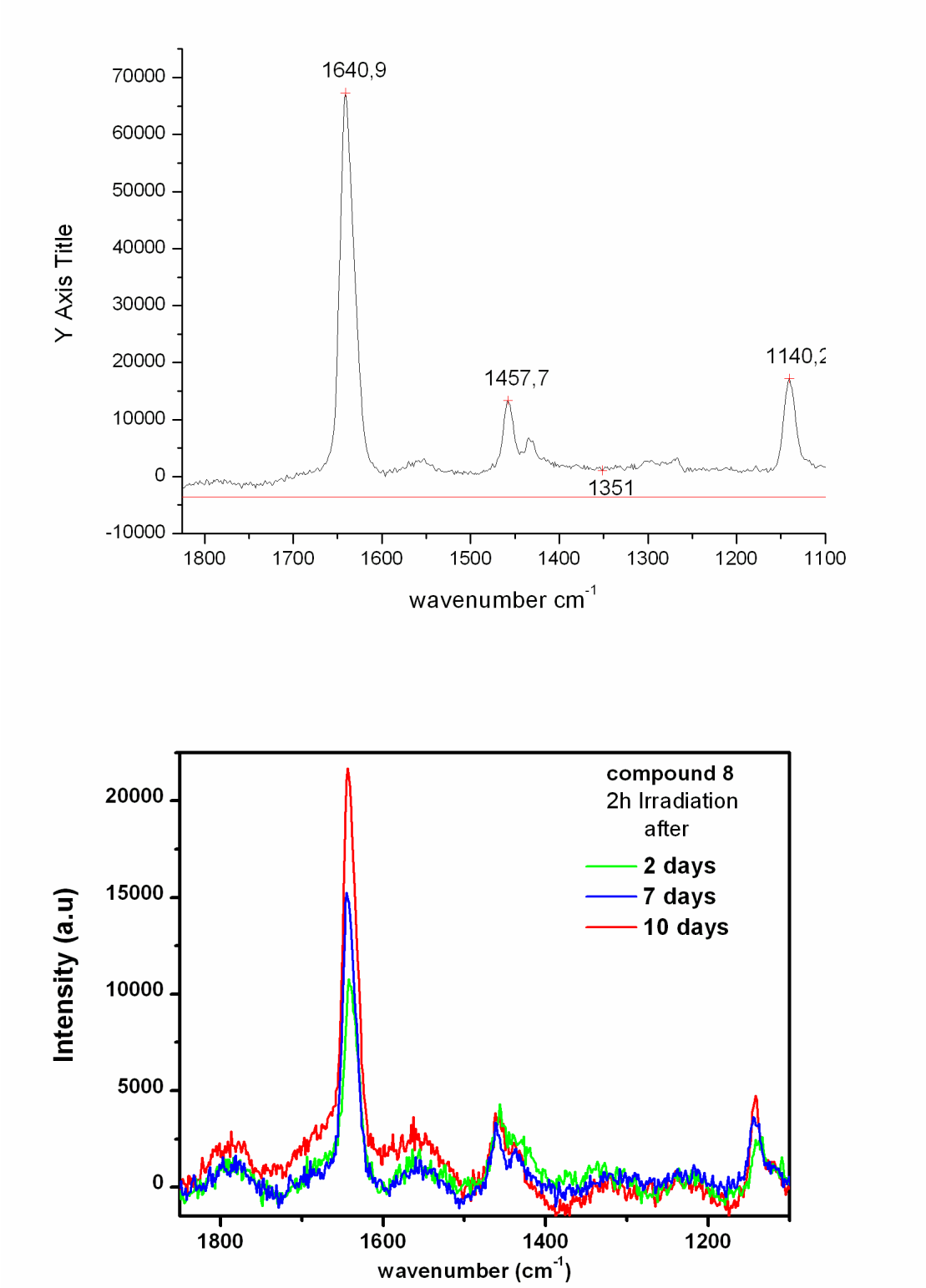

Figure S16. Solid state Raman spectrum of compound **8** before irradiation (up). Raman spectra of compound **8** irradiated for 2h, obtained at different time intervals (down).

Electronic Supplementary Material (ESI) for Chemical Communications